

Journal of Biomedical Optics

SPIEDigitalLibrary.org/jbo

Near-infrared diffuse optical monitoring of cerebral blood flow and oxygenation for the prediction of vasovagal syncope

Ran Cheng
Yu Shang
Siqi Wang
Joyce M. Evans
Abner Rayapati
David C. Randall
Guoqiang Yu

Near-infrared diffuse optical monitoring of cerebral blood flow and oxygenation for the prediction of vasovagal syncope

Ran Cheng,^a Yu Shang,^a Siqi Wang,^a Joyce M. Evans,^a Abner Rayapati,^b David C. Randall,^{a,c} and Guoqiang Yu^{a,*}

^aUniversity of Kentucky, Department of Biomedical Engineering, Lexington, Kentucky 40506

^bUniversity of Kentucky, Department of Psychiatry, Lexington, Kentucky 40509

^cUniversity of Kentucky, Department of Physiology, Lexington, Kentucky 40536

Abstract. Significant drops in arterial blood pressure and cerebral hemodynamics have been previously observed during vasovagal syncope (VVS). Continuous and simultaneous monitoring of these physiological variables during VVS is rare, but critical for determining which variable is the most sensitive parameter to predict VVS. The present study used a novel custom-designed diffuse correlation spectroscopy flow-oximeter and a finger plethysmograph to simultaneously monitor relative changes of cerebral blood flow (rCBF), cerebral oxygenation (i.e., oxygenated/deoxygenated/total hemoglobin concentration: $r[\text{HbO}_2]/r[\text{Hb}]/r\text{THC}$), and mean arterial pressure (rMAP) during 70 deg head-up tilt (HUT) in 14 healthy adults. Six subjects developed presyncope during HUT. Two-stage physiological responses during HUT were observed in the presyncopal group: slow and small changes in measured variables (i.e., Stage I), followed by rapid and dramatic decreases in rMAP, rCBF, $r[\text{HbO}_2]$, and rTHC (i.e., Stage II). Compared to other physiological variables, rCBF reached its breakpoint between the two stages earliest and had the largest decrease ($76 \pm 8\%$) during presyncope. Our results suggest that rCBF has the best sensitivity for the assessment of VVS. Most importantly, a threshold of $\sim 50\%$ rCBF decline completely separated the subjects from those without presyncope, suggesting its potential for predicting VVS. © 2014 Society of Photo-Optical Instrumentation Engineers (SPIE) [DOI: 10.1117/1.JBO.19.1.017001]

Keywords: cerebral blood flow; cerebral oxygenation; diffuse correlation spectroscopy; near-infrared spectroscopy; vasovagal syncope.

Paper 130659R received Sep. 12, 2013; revised manuscript received Dec. 1, 2013; accepted for publication Dec. 10, 2013; published online Jan. 8, 2014.

1 Introduction

Syncope, a transient loss of consciousness and postural tone, is responsible for up to 6% of hospital admissions and 3% of emergency department visits across the United States.^{1,2} Although the mortality rate of syncope is low,³ the sudden loss of consciousness due to syncope can be fatal and may endanger the public, for example, during driving or flying. Sorajja et al. reported that among subjects evaluated for syncope from 1996 to 1998 at Mayo Clinic, 9.8% had at least one syncopal episode while driving.⁴ For pilots in high performance aircraft, the high gravity force during training/duty pools blood to the lower body resulting in cerebral hypoperfusion and hypoxia, which may lead to syncope. According to Carter et al., up to 48% of the United State Air Force population has experienced syncope.⁵ Developing criteria for early predication of syncope may avoid actual syncope and any consequential accident.

The head-up tilt (HUT) test has been widely used for the study of vasovagal syncope (VVS), the most commonly occurring syncope. HUT may generate central hypovolaemia^{6,7} and increase sympathetic outflow⁷ that eventually result in a vasovagal reaction. The vasovagal reaction is a malfunctioning of the autonomic nervous system that initiates decreases in blood pressure, heart rate (HR), and cerebral blood flow (CBF), possibly leading to VVS even in healthy volunteers. Although the pathophysiology of the vasovagal reaction is not fully known,

the sudden drops in arterial blood pressure (ABP), blood flow velocity in the middle cerebral artery (MCA), and cerebral oxygenation have been previously observed during presyncope⁸ and VVS.⁹ Continuous and simultaneous monitoring of these physiological variables during presyncope/VVS is rare, but critical for determining which variable is the most sensitive parameter to predict VVS. Also, prediction of VVS is crucial for preventing VVS.

Transcranial Doppler ultrasound (TCD) and near-infrared spectroscopy (NIRS) have been broadly used in the noninvasive study of presyncope⁸ and VVS.⁹⁻¹¹ TCD measures cerebral blood flow velocity (CBFV) in major arteries (e.g., MCA) through a transcranial Doppler window where the skull bones are relatively thin. However, CBFV in large vessels may not accurately reflect blood flow in cerebral microvasculature.¹² In addition, approximately 9% of adults are not candidates for TCD measurements due to their poor acoustic windows.¹³ Conventional NIRS evaluates cerebral blood oxygenation based on the difference in near-infrared (NIR) absorption spectra of major tissue chromophores, i.e., oxygenated hemoglobin (HbO_2) and deoxygenated hemoglobin (Hb).¹⁴ In contrast to TCD, NIRS measurement is sensitive to cerebral oxygenation in small vessels of the cerebral cortex. Although some research groups combined TCD and NIRS measurements in the study of presyncope¹⁵ and VVS.¹⁶ CBFV and cerebral oxygenation were

*Address all correspondence to: Guoqiang Yu, E-mail: guoqiang.yu@uky.edu

not measured from the same region of brain in these studies. Single photon emission computed tomography (SPECT) has also been used to evaluate the regional difference of CBF in small vessels during VVS induced by HUT.¹⁷ However, low temporal resolution and high cost limit its clinical application. Furthermore, SPECT involves exposure to ionizing radiation.

Since the sudden drop of blood pressure is well known to be a sign for developing VVS, ABP parameters, such as mean arterial pressure (MAP),^{2,15} systolic and diastolic blood pressures,¹⁸ and beat-to-beat blood pressure waveform,⁸ have been continuously monitored in the previous studies of presyncope and VVS using a noninvasive finger plethysmograph or an invasive catheter.^{2,8,15} To determine which variable can be used to predict the oncoming VVS, previous studies have simultaneously measured ABP and CBFV during presyncope² or ABP and cerebral oxygenation during VVS¹⁸ and found that rapid declines in cerebral hemodynamics occurred earlier than the decreases in ABP. To date, very few studies have simultaneously quantified dynamic changes of ABP, CBFV, and cerebral oxygenation during presyncope¹⁵ and VVS,¹⁶ and none of those few was intended to determine quantitatively which parameter predicted the oncoming VVS.

A novel NIR dual-wavelength diffuse correlation spectroscopy (DCS) flow-oximeter developed recently in our laboratory offers a noninvasive, fast, portable, and low-cost tool for simultaneously monitoring the relative changes of blood flow and blood oxygenation in the same tissue region of interest.¹⁹⁻²¹ DCS for blood flow measurement has been extensively validated against other techniques in various organs/tissues, including Doppler ultrasound in premature infant brain,²² power spectral Doppler ultrasound in murine tumors,²³ laser Doppler flowmetry in mouse brains,²¹ fluorescent microsphere measurement of CBF in piglet brain,²⁴ ASL-MRI in human muscle,²⁵ and Xenon computed tomography in traumatic brain,²⁶ while DCS flow-oximeter for oxygenation measurement has been validated against commercial NIRS oximeter (Imagent, ISS Inc., Champaign, Illinois).¹⁹ In this study, we used a finger plethysmograph and a custom-designed DCS flow-oximeter to concurrently monitor the blood pressure and dynamic changes of CBF, concentrations of HbO₂ ([HbO₂]), Hb ([Hb]) and total hemoglobin (THC) in healthy subjects during 70 deg HUT tests. MAP was reported in this study since it quantified arterial pressure responses in a single value that was sensitive to both systolic and diastolic pressures. HUT was used to challenge physiological maintenance of constant MAP, CBF, and cerebral oxygenation. Instability of these variables may induce VVS. The ultimate goal was to quantify dynamic changes in multiple physiological variables (i.e., MAP, CBF, [HbO₂], [Hb], and THC) during postural change (HUT) and to assess their sensitivities to predict VVS.

2 Methods

2.1 Participants

Fourteen healthy adults (six males and eight females) without known cerebral or cardiac diseases participated in this study (Table 1) after signing consent forms approved by the University of Kentucky Institutional Review Board. These subjects were subdivided according to the response to HUT; a control group with negative HUT response (eight subjects) and a presyncopal group (six subjects) with positive HUT response who experienced presyncope (i.e., sudden drop in blood

pressure, dizziness, blurred vision, sweating, and heart palpitation) during 70 deg HUT.

2.2 HUT Protocol

The subject was asked to lay supine on a tilt table. Two Velcro strips were placed over the chest and thighs to secure the body to the tilt table. After acquiring supine control for ~10 min, the subject was tilted up to 70 deg and instructed to remain still for 30 min. However, if presyncopal symptoms appeared during standing at 70 deg, the subject was tilted back immediately to supine position for recovery. Therefore, none of the subjects experienced syncope during the test for safety reasons. A recovery period of ~5 min was then followed at supine position. This HUT protocol was selected because the previous studies had shown that it may induce presyncope in healthy subjects.²⁷

2.3 DCS Flow-Oximeter for Cerebral Hemodynamic Measurement

A custom-designed dual-wavelength DCS flow-oximeter was used to detect the relative changes of CBF, [HbO₂], [Hb], and THC during HUT. The details about the DCS flow-oximeter can be found elsewhere.¹⁹⁻²¹ Briefly, long-coherence length (>5m) NIR lights generated by two continuous-wave laser diodes (785 and 854 nm, 100 mW, CrystaLaser Inc., Reno, Nevada) were delivered alternately to tissues via two multimode source fibers (core diameter of each fiber = 200 μm, emission area = 0.13 mm²) bundled tightly together. Each laser was switched on for 450 ms with a 50-ms interval for the transition between the two lasers. Thus data sampling time for one complete frame was 1 s. Photons transported through the tissue were either scattered by tissue scatterers [e.g., red blood cells (RBCs), organelles, and mitochondria] or absorbed by tissue absorbers (e.g., hemoglobin). Only some photons were eventually collected by four detector fibers bundled together (core diameter of each fiber = 5.6 μm, detection area of four fibers = 0.32 mm²). Tissue heterogeneities at the small emission and detection areas were minor and can be ignored.¹² The detector fibers were connected to four single-photon-counting avalanche photodiodes (APDs, Excelitas Technologies Corp., Waltham, Massachusetts). The signals from the four APDs were averaged to increase the signal-to-noise ratio. The source and detector fibers were placed on the tissue surface with a distance between them of millimeters to centimeters, depending on the desired penetration depth of light. Photon diffuse theory holds that the penetration depth of NIR light in biological tissues is approximately one-half of the source-detector (S-D) separation.²⁸ In this study, we used a fiber-optic probe with the S-D separation of 2.5 cm. This separation allowed for the detection of cerebral hemodynamics in the adult prefrontal cortex.^{12,20}

The blood flow measurement was achieved by monitoring the light intensity fluctuations in a single speckle area covered by the single-mode fiber in the tissue surface. Fluctuations detected by the APDs resulted from the motion of moving scatterers, primarily RBCs in tissue microvasculature. A four-channel correlator (correlator.com, Bridgewater, New Jersey) was used to calculate the normalized light intensity temporal autocorrelation functions (g_2) from the outputs of APDs. According to the Siegert relation,²⁹ the normalized electric field temporal autocorrelation function (g_1) can be derived from the measured g_2 . The unnormalized electric field temporal autocorrelation function (G_1) satisfies the correlation diffusion equation in

Table 1 Subject characteristics.

Subject	Sex	Age (years)	Values at supine		HUT Duration (min)	Valid measurements during HUT		
			MAP (mm Hg)	HR (BPM)		MAP (%)	CBF (%)	Oxygenation (%)
Presyncopal group ($N = 6$)								
S1	F	57	95	70	15.4	✓	✓	✓
S2	F	60	105	62	2.7	N/A	✓	N/A
S3	F	60	81	71	10.6	✓	✓	N/A
S4	F	39	82	77	5.9	✓	✓	✓
S5	M	40	72	58	2.5	✓	✓	✓
S6	M	24	96	50	9.3	✓	✓	✓
Control group ($N = 8$)								
C1	M	47	83	67	30.0	✓	✓	✓
C2	M	55	77	70	30.0	✓	✓	✓
C3	M	59	79	65	30.0	✓	✓	✓
C4	F	51	95	77	30.0	✓	✓	✓
C5	F	48	85	80	30.0	✓	✓	✓
C6	F	46	75	61	30.0	✓	✓	✓
C7	F	33	87	66	30.0	✓	✓	✓
C8	M	26	80	63	30.0	✓	✓	✓
Average age, supine MAP and HR, and HUT duration			Age (years)	Supine MAP (mm Hg)	Supine HR (BPM)	HUT Duration (min)		
Presyncopal group ($N = 6$)			46.7 ± 14.7	88.5 ± 12.2	64.7 ± 9.9	7.7 ± 5.0		
Control group ($N = 8$)			45.6 ± 11.0	82.6 ± 6.4	68.6 ± 6.7	30.0 ± 0.0		
All groups ($N = 14$)			46.1 ± 12.2	85.1 ± 9.4	66.9 ± 8.1	20.5 ± 11.8		

highly scattering media.³⁰ For the diffusive motion of RBCs in tissue microvasculature, the mean-square displacement of moving RBCs in time τ is $\langle \Delta r^2(\tau) \rangle = 6D_B\tau$, where D_B is the effective diffusion coefficient of the moving RBCs. Since not all scatterers in tissue are dynamic, an α term (0 to 1) is added and defined as the ratio of moving scatterers to total scatterers.³⁰ The blood flow index in biological tissues is then represented by the combined term αD_B which is derived by fitting the autocorrelation function g_1 to its analytical solution of correlation diffusion equation.^{21–26} Although the unit of αD_B (cm^2/s) is different from the classical blood flow unit in tissues ($\text{ml}/\text{min}/100 \text{ ml}$), relative changes in αD_B have been found to correlate well with the blood flow changes measured by other established modalities.^{21–26,31,32}

The oxygenation information was extracted from the changes in average light intensities at the two wavelengths (785 and 854 nm) detected by the APDs. Using the known extinction coefficients of major chromophores (i.e., HbO_2 and Hb) and differential path length factors (DPFs) at corresponding wavelengths,¹⁴ the modified Lambert–Beer law was applied to determine relative changes of $[\text{HbO}_2]$ and $[\text{Hb}]$ in a unit

of $\mu\text{mol}/\text{L}$ from the measured light intensities. $\Delta[\text{HbO}_2]$ and $\Delta[\text{Hb}]$ represent the subtracted differences between the time course data and their baselines (assigned to be “0”), respectively.

2.4 Data Collection

For the optical measurements of cerebral hemodynamic parameters, the fiber-optic probe described above was taped in the middle of forehead at the position of 1 cm above the eyebrows. A self-adhesive elastic band was then employed around the forehead to fix the probe tightly and minimize the influence of room light on optical measurements. The beat-to-beat MAP in units of mm Hg and HR in units of beats-per-minute (BPM) were monitored continuously via a noninvasive finger plethysmograph (Portapres, FMS Inc., Amsterdam, Netherlands). The plethysmograph sensor was fixed on the middle finger of the left hand and maintained at heart level. Optical and MAP/HR data were continuously recorded throughout the HUT protocol at a sampling rate of 1 Hz.

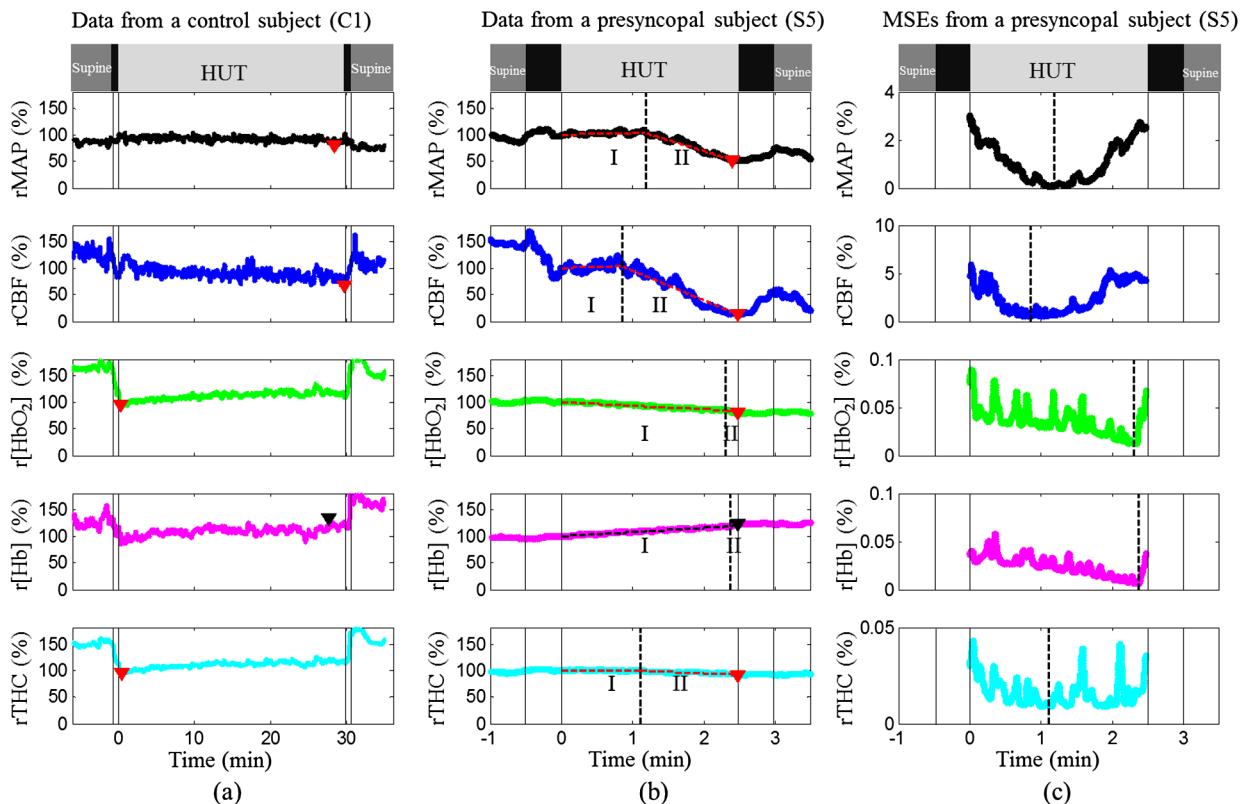


Fig. 1 MAP and cerebral hemodynamics from a control subject (a) and a presyncopal subject (b), and corresponding MSEs of the two-line linear fittings in a subject with presyncope (c). During HUT, all the measured variables were relatively stable in the control subject (C1) but exhibited two-stage physiological responses in the subject (S5) with presyncope (i.e., slow and gradual changes at Stage I and rapid and dramatic changes at Stage II). The solid vertical lines indicate the beginning and ending of tilting up and tilting down. The triangles indicate the minima of rMAP, rCBF, r[HbO₂], and rTHC and the maximum of r[Hb] during HUT. The two connected dashed lines on the top of the raw data (b) demonstrate the two-line fitting results. The dashed vertical lines indicate the breakpoints separating the Stage I and Stage II.

2.5 Data Analysis

A 10-point sliding average was applied on all the raw data to reduce the high frequency noise. The supine MAP and HR were fairly stable, thus the averaged data from the 30 s immediately before the onset of HUT were used to represent their baseline values at the supine position. In order to compare HUT-induced changes among parameters with different units, all measured variables (i.e., MAP, αD_B , $\Delta[\text{HbO}_2]$, $\Delta[\text{Hb}]$, ΔTHC) were normalized (divided), respectively, to the averaged values of the 30-s data segment immediately after the tilting table was positioned at 70 deg. rMAP, rCBF, r[HbO₂], r[Hb], and rTHC represent the relative values normalized (divided) by their baseline values, respectively. For the calculation of r[HbO₂], r[Hb], and rTHC, baseline values of these variables were assigned to be 23.6, 13.0, and 37.5 $\mu\text{mol/L}$, respectively, based on the literature.³³ After normalization, all baselines were assigned to be 100%.

Similar to observations made in the previous studies,^{2,8,16} subjects with presyncope exhibited two stages of physiological responses during HUT (see Figs. 1 and 2 in Sec. 3): (1) a slow and gradual change in each measured variable at Stage I before a breakpoint and (2) rapid and dramatic changes at Stage II after the breakpoint. The maximum changes in all measured variables occurred at Stage II in presyncopal subjects. To compare sensitivities of the measured variables for predicting VVS, we

determined the minimum values of rMAP, rCBF, r[HbO₂], and rTHC and maximum of r[Hb] during HUT in control and presyncopal subjects. We also calculated the onset time of rapid/dramatic dynamic changes before presyncope following the method suggested by Dan et al. in presyncopal subjects.² Briefly, the dynamic time course data during HUT for each parameter were fitted by two straight lines (i.e., linear least squares fit) that represented the slow and rapid changes, respectively.² A breakpoint connecting the two straight lines [see Figs. 1(b) and 2(a)] was moved from the beginning to the end of HUT along each data set, and the corresponding mean squared errors (MSEs) of the linear best fits were calculated. The final breakpoint separating the two stages was chosen at the time point where the smallest MSE was achieved. For comparisons, the time differences of breakpoints between the rMAP and each of the other hemodynamic parameters (i.e., rCBF, r[HbO₂], r[Hb], rTHC) were quantified.

One-way analysis of variance (ANOVA) was used to test the differences of maximum physiological changes during HUT between the presyncopal and control groups, and the differences in the times required to reach to the breakpoints among rMAP, rCBF, r[HbO₂], r[Hb], and rTHC (relative to rMAP) in the presyncopal subjects. The differences were considered significant for p -values < 0.05 . All average results are presented as mean \pm standard deviation (SD).

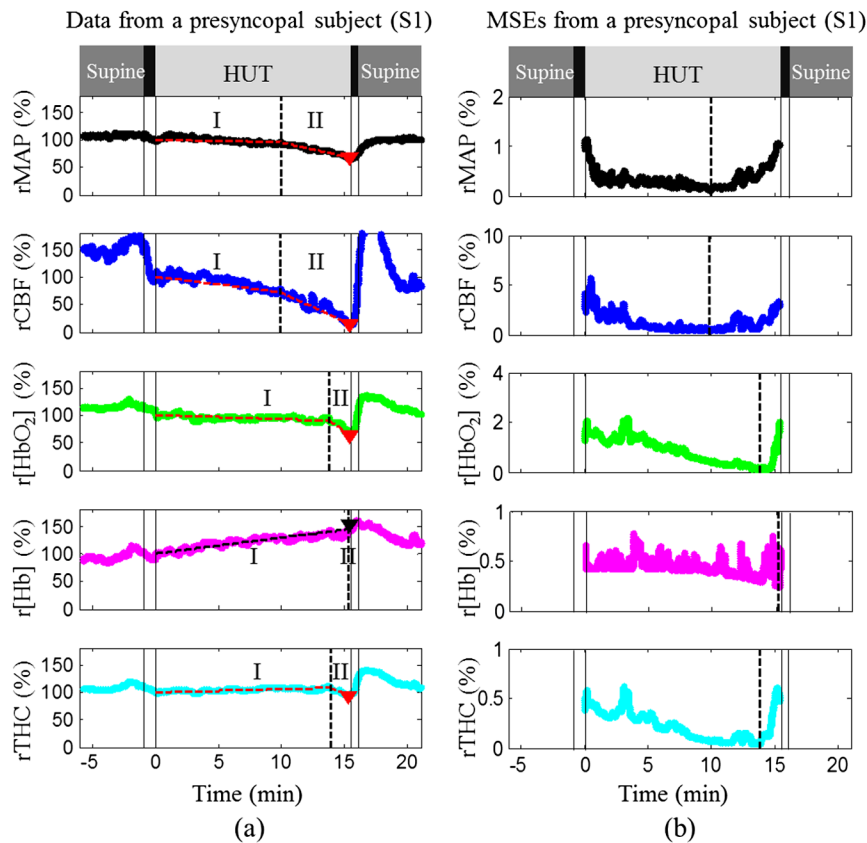


Fig. 2 MAP and cerebral hemodynamics during HUT (a) and corresponding MSEs of the two-line linear fittings (b) in a subject with presyncope (S1). All symbols and lines in this figure represent the same meanings as those used in Fig. 1. Physiological response trends to HUT in this subject were similar to those shown in Fig. 1(b) although large variations existed between them in terms of how much and how fast these changes were.

3 Results

3.1 Characterization of Participants

In this study, six subjects developed presyncope during the 30-min HUT test (see Table 1). The average time from the beginning of tilting to the onset of presyncope was 7.7 ± 5.0 min in the presyncopal group. We excluded the MAP data from one subject with presyncope (S2) due to the measurement artifact indicated by huge variations with some negative values (-300 to 1000 mm Hg). Oxygenation data from two subjects with presyncope (S2 and S3) were not available because one of the lasers in the DCS flow-oximeter was not working properly during the measurements. There were no significant differences between the presyncopal and control groups in age, supine MAP, and HR before tilting.

3.2 Individual Responses During HUT

Figure 1 shows data illustrative of MAP and cerebral hemodynamics from a control subject (C1 in Table 1) without presyncope [Fig. 1(a)], and a subject (S5 in Table 1) with presyncope [Fig. 1(b)] and corresponding MSEs of the two-line fittings [Fig. 1(c)]. All measured variables from the two subjects exhibited sudden changes at the onset of HUT [Figs. 1(a) and 1(b)]. During HUT, all variables measured from the control subject (C1) were relatively stable [Fig. 1(a)] and therefore showed

no two-stage responses. The minima of rMAP, rCBF, r[HbO₂], and rTHC in the control subject (C1) were 85%, 68%, 96%, and 95% of the 30-s mean value immediately after tilt-onset (assigned to be 100%), respectively, and the maximum r[Hb] was 129% [Fig. 1(a)]. By contrast, most variables measured from the subject with presyncope (S5) showed relatively larger changes. The rCBF decrease during HUT was associated with a decrease in r[HbO₂] and an increase in r[Hb]. The rTHC primarily followed the trend of r[HbO₂] since [HbO₂] accounts for >60% of the THC in CBF (i.e., as opposed to [Hb]).³⁴ Two stages of physiological responses were observed during HUT including slow and gradual changes in the measured variables during Stage I, and rapid and dramatic changes during Stage II. The breakpoint for each parameter between the two stages was determined mathematically by the minimum value of MES, although the nadirs of MSEs were not always obvious in all measured parameters. The maximum changes during HUT occurred at Stage II. The minimum value of rCBF (15%) was much smaller than those of rMAP (52%), r[HbO₂] (80%), and rTHC (92%). The maximum r[Hb] was 123%. The onset times of rapid changes in rCBF, r[HbO₂], r[Hb], and rTHC at the breakpoints were -20 , $+68$, $+72$ and -4 s relative to that of rMAP, respectively [Figs. 1(b) and 1(c)]. The negative or positive value of each onset time indicated that the rapid and dramatic change of the measured parameter occurred earlier or later than that of rMAP (as a reference for the comparison).

We observed similar trends from all subjects with presyncope although large intersubject variations existed among these subjects. Figure 2 shows the data from another subject (S1 in Table 1) with presyncope. Note that the time scales in horizontal axes of Figs. 1 and 2 were not the same due to the difference in HUT durations. Similarly, the minimum value of rCBF (15%) at Stage II was much smaller than those of rMAP (67%), r[HbO₂] (65%), and rTHC (94%). The maximum value of r[Hb] was 150%. All the variables changed gradually before the breakpoints at Stage I and rapidly thereafter at Stage II. The onset times of rCBF, r[HbO₂], r[Hb], and rTHC at the breakpoints were -3, +231, +320 and +234 s relative to that of rMAP, respectively. It should be noticed that the rMAP and rCBF demonstrated the two stages of dynamic changes more obviously than the other variables, and rCBF decreased greater and earlier at Stage II than the other parameters in the subjects with presyncope (Figs. 1 and 2).

3.3 Average Results

Figure 3 displays the minimum values of rMAP, rCBF, r[HbO₂], and rTHC and maximum values of r[Hb] during HUT measured from the subjects with valid data. The mean minimum values of rMAP (61 ± 19%), rCBF (24 ± 8%), and r[HbO₂] (64 ± 12%) in the presyncope group were significantly lower than those in the control group ($p < 0.05$, one-way ANOVA). Among these three parameters (i.e., rMAP, rCBF, r[HbO₂]), however, only the minimum values of rCBF (24 ± 8%) exhibited a clear threshold (~50%) to separate all the individuals in the presyncope group (range: 15% to 35%) from all subjects in the control group (range: 57% to 85%). The time durations from rCBF reaching the threshold of 50% decline to the occurrence of presyncope were 80 ± 79 s (range: 14 to 224 s). In addition, there were no significant differences in maximum r[Hb] and minimum rTHC between the two groups.

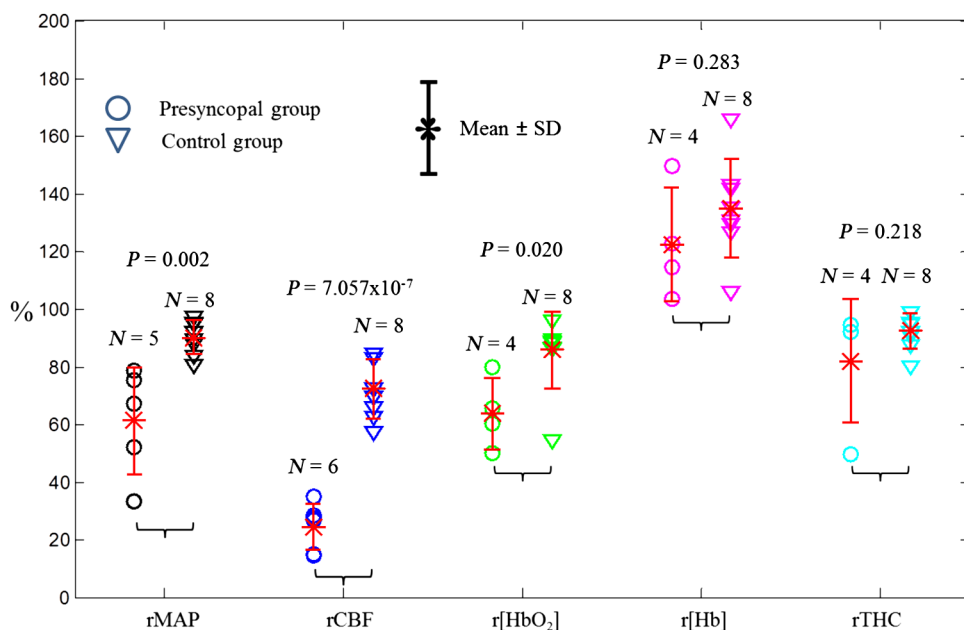


Fig. 3 Distributions of maximum r[Hb] and minimum rMAP, rCBF, r[HbO₂], and rTHC in presyncope and control groups. The circles and triangles represent individuals with and without presyncope, respectively. The asterisks with error bars represent the group means ± standard deviations.

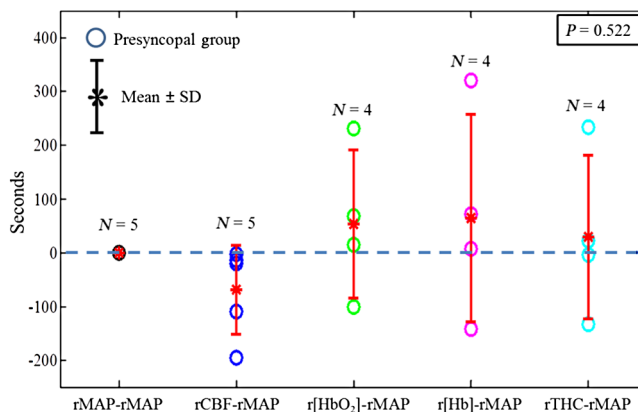


Fig. 4 Onset time differences at the breakpoints of rMAP, rCBF, r[HbO₂], r[Hb], and rTHC relative to rMAP in the presyncope group. The asterisks with error bars represent the group means ± standard deviations. The dashed horizontal line represents 0 s. The negative/positive value below/above the dashed horizontal line (0 second) indicates that the breakpoint of cerebral hemodynamic parameters (i.e., rCBF, r[HbO₂], r[Hb], and rTHC) occurred earlier/later than that of rMAP.

Figure 4 shows the time differences at the breakpoints in rMAP, rCBF, r[HbO₂], r[Hb], and rTHC relative to rMAP in the presyncope group. Among all hemodynamic variables only rapid changes of rCBF after the breakpoints occurred consistently earlier (range: 3 to 195 s) than those of rMAP in all subjects with presyncope. On average, the breakpoints for all the variables occurred in the sequence of rCBF (-68 ± 82 s), rMAP (0 s), rTHC (30 ± 152 s), r[HbO₂] (53 ± 138 s), and r[Hb] (64 ± 192 s) when using rMAP as the reference (0 s). However, due to the large data variation and small number of subjects, these time differences at the breakpoints were not significantly different ($p = 0.522$, one-way ANOVA).

4 Discussion and Conclusions

Direct and concurrent measurement of dynamic changes in CBF and cerebral oxygenation during VVS is crucial because the cerebral hypoperfusion and hypoxia are the causes of losses of consciousness and postural tone during VVS.^{8,9} A device for noninvasive measurement of both CBF and cerebral oxygenation is appealing for predicting VVS. The emerging DCS flow-oximeter is a portable, rapid, and relatively inexpensive device which can continuously and concurrently monitor CBF and cerebral oxygenation during on-going tests.^{19–21} This paper reports the first noninvasive and continuous monitoring of both CBF and cerebral oxygenation within the same region of the brain cortex during presyncope using the novel dual-wavelength DCS flow-oximeter. We found that among all the measured variables (i.e., rMAP, rCBF, r[HbO₂], r[Hb], rTHC), rCBF has the best sensitivity for predicting VVS.

In this study, larger variations in MAP and cerebral hemodynamics during HUT were observed in subjects with presyncope [see Figs. 1(b) and 2(a)] compared to the controls without presyncope [see Fig. 1(a)]. More specifically, MAP, CBF, [HbO₂], and THC decreased while [Hb] increased during HUT; such changes are consistent with the results from the previous studies.^{8,10,16,18}

The presyncopal group showed two-stage physiological responses during HUT: slow and gradual changes before the breakpoints at Stage I, and rapid and dramatic changes after the breakpoints at Stage II [see Figs. 1(b) and 2(a)]. The average durations of Stage II for all measured parameters ranged from 64 to 167 s. Thus, the sampling time of 1 s used in the present measurements was short enough to track rapid dynamic changes at Stage II. Other groups also observed similar two-stage responses in MAP, CBFV, and [HbO₂] during presyncope^{2,8,15} and VVS^{16,18} induced by HUT.^{2,8,15,16,18} These changes were expected as HUT induced gradual decreases in MAP and CBF at Stage I which led to gradual decreases in [HbO₂] and THC as well as a gradual increase in [Hb]. These gradual and slow changes then reached the critical breakpoints leading to Stage II during which physiological autoregulation eventually failed to prevent the observed sharp dynamic changes in the measured variables. We also found that the maximum changes of all physiological variables occurred after the breakpoints at Stage II. Taken together, it is reasonable to conclude that the sharp and large physiological changes at Stage II result in the oncoming presyncope.

Among all the measured variables, rCBF had the largest changes (76 ± 8% decline) at Stage II compared to rMAP (38 ± 19% decline), r[HbO₂] (36 ± 64% decline), rTHC (18 ± 22% decline), and r[Hb] (22 ± 20% increase) in subjects with presyncope (see Fig. 3), suggesting that rCBF has the best sensitivity for the assessment of VVS. Njemanze also found similar results in subjects with VVS induced by HUT; the percentage maximum drops of mean CBFV (58 ± 14%) in MCA were much larger than the decreases in systolic (37 ± 23%) and diastolic (32 ± 20%) blood pressures during VVS.³⁵ In another study, Schondorf et al. observed a significant decrease of diastolic CBFV (~40%) in MCA.³⁶ Apparently, the maximum CBF decreases (76 ± 8%) in microvasculature found in the present study were larger than the maximum drops of mean CBFV (58 ± 14%)³⁵ or diastolic CBFV (~40%)³⁶ in MCA measured by Doppler ultrasound, implying that CBF in small vessels may be more sensitive than CBFV in large vessels for the assessment of VVS. In addition, Joo et al. reported that CBF

in small vessels of the right prefrontal cortex measured by SPECT during HUT was negatively correlated to the total number of syncopal episodes,¹⁷ which had been demonstrated to be the most powerful predictor of a future syncope.³⁷ Therefore, CBF measurement holds potential to evaluate the recurrence rate of VVS.

The most important finding in the present study was the threshold of ~50% rCBF decrease during HUT, which can be used to completely separate the control and presyncopal groups (see Fig. 3). Potentially, real-time continuous monitoring of CBF may provide prognostic information for the occurrence of VVS, i.e., a >50% CBF decrease may result in VVS. Although Njemanze also suggested that a ~50% drop of mean CBFV in MCA was the critical limit to maintain consciousness, there were overlaps in CBFV data across the control and syncope groups with this threshold of 50% CBFV drop.³⁵ Furthermore, we found that the time durations from rCBF reaching the threshold of 50% decline to the occurrence of presyncope were 80 ± 79 s (range: 14 to 224 s). It has been reported that presyncope occurs about 2 min before the expression of syncope symptoms.¹⁸ Therefore, detection of the early decrease in rCBF to 50% provides a time window of >2 min for predicting/preventing VVS.

Compared to other measured variables, rCBF reached the breakpoint earlier (see Fig. 4), although the time differences at breakpoints were not statistically significant. For example, the breakpoint of rCBF occurred 68 ± 82 s (range: 3 to 195 s) ahead of rMAP. The lack of significance is likely due to the small number of subjects and large variations in time differences (i.e., 68 ± 82 s). Nevertheless, our findings are consistent with the results from the study of Dan et al., where the CBFV decreases were found to significantly lead the MAP reductions by 67 s (range: 9 to 197 s).² The earlier changes in CBF or CBFV compared to other physiological variables suggest that the cerebral hypoperfusion at Stage II after the breakpoint may be the primary cause of the sharp changes in other physiological parameters. The right insular cortex is known to be responsible for regulating sympathetic activities such as HR and blood pressure.^{10,17} It is possible that reduced CBF in the right insular cortex suppresses sympathetic activities, eventually leading to VVS.¹⁷

As expected, cerebral hypoperfusion (i.e., CBF decline) occurred during presyncope along with cerebral hypoxia (i.e., [HbO₂] decrease and [Hb] increase). Among all measured cerebral oxygenation variables, only the minimum values of r[HbO₂] during HUT were significantly different between the control and presyncopal groups (86 ± 13% versus 64 ± 12%, $p = 0.020$, one-way ANOVA, see Fig. 3). This is likely due to the relatively larger changes in r[HbO₂] (compared to r[Hb] and rTHC) during presyncope observed in the present study (see Fig. 3) as well as from the previous other investigations.^{16,18} Moreover, due to the relatively smaller changes in r[HbO₂], r[Hb], and rTHC compared to other measured variables (i.e., rMAP and rCBF) their breakpoints were not always obvious during presyncope [see Fig. 1(b)]. This resulted in large variations in time differences determined at the breakpoints (see Fig. 4), and possibly led to evaluation errors.

The present study investigated relationships among the changes of cerebral hemodynamics and MAP during presyncope. In fact, the control of cerebral hemodynamics also involves systemic hemodynamic and metabolic factors. For example, CBF is very sensitive to changes in arterial CO₂

content via changes in respiration. Ideally, investigation of cerebrovascular responses should also include assessment of CO₂ levels (e.g., End Tidal CO₂) and/or ventilation/respiratory rate to quantify the effects of reductions in CO₂ and hyperventilation on CBF independent of changes in MAP.³⁸ CO₂ measurements will be included in the future studies and different types of VVS (i.e., vasodepressor, cardioinhibitory, and mixed) will be investigated in large clinical populations.

Another concern for this study was the influence of overlying tissues (skin and skull) on NIR DCS flow-oximeter measurements of cerebral hemodynamics. Monte Carlo simulations of NIR light paths in the human brain have demonstrated that the S-D separation of 2.5 cm used in the present study can detect the cerebral hemodynamics in the prefrontal cortex.³⁹ Furthermore, the use of 2.5 cm S-D separation for DCS measurements was demonstrated and validated previously in human brains.^{12,20} Nevertheless, there were always some contributions to the cortex signal from overlying tissues (skin and skull tissues), i.e., the partial volume effect.³¹ For example, sudden cerebral hemodynamic changes were detected immediately after tilting in both presyncopal and control subjects as shown in Figs. 1 and 2. Although other groups also observed sudden changes in CBFV (Ref. 8) and cerebral oxygenation¹⁶ and attributed them to circulatory responses induced by orthostatic stress, the skin fluid (including blood) shift from head to lower body induced by gravity during the transition of tilting could also contribute to our optical measurements, leading to overestimation of cerebral responses. Future study will use the optical probe with multiple S-D separations to detect hemodynamic responses in different tissue layers as well as multilayer theoretical models⁴⁰ to correct the influence of overlying tissues on cerebral hemodynamic measurements.

In summary, we have utilized a novel DCS flow-oximeter and a finger plethysmograph to noninvasively and continuously monitor dynamic changes in blood pressure (rMAP) and cerebral hemodynamics (i.e., rCBF, r[HbO₂], r[Hb], and rTHC) during 70 deg HUT in healthy subjects with or without presyncope. The main focus of this preliminary study is to show the capability of our novel device to detect physiological responses in presyncopal episodes. Notably, even with a small sample size, we were still able to detect a significant decrease in rCBF at the onset of presyncope.

Specifically, all measured physiological parameters were relatively stable during HUT in the control group without presyncope. By contrast, the presyncopal group had slow and gradual changes at Stage I before the breakpoints, and rapid and dramatic changes at Stage II after the breakpoints: continuous decreases in rMAP, rCBF, r[HbO₂], and rTHC, and an increase in r[Hb]. Among all measured variables, rCBF reached the breakpoint at earliest time and had the largest decrease at Stage II, suggesting the best sensitivity of rCBF for the assessment of VVS. Most importantly, this study found a threshold of ~50% rCBF decrease which can potentially be used to predict the occurrence of VVS. In addition, simultaneous measurements of CBF and cerebral oxygenation in the present study revealed that the cerebral hypoperfusion (i.e., CBF decline) was associated with the cerebral hypoxia (i.e., r[HbO₂] decrease and r[Hb] increase) during presyncope. Ultimately, such information may be used for warning subjects at high risk for the recurrence of VVS, or even preventing VVS via an automatic feedback (e.g., an antigravity suit used for Air Force pilots) to maintain cerebral hemodynamics in a normal level.

Acknowledgments

We acknowledge the support from the National Institutes of Health R01 NS039774-04-07 (D.C.R.), R01 CA149274 (G.Y.), and R21 AR062356 (G.Y.). We also thank Daniel Irwin for his help in preparing the manuscript.

References

- H. Calkins et al., "The economic burden of unrecognized vasodepressor syncope," *Am. J. Med.* **95**(5), 473–479 (1993).
- D. Dan et al., "Cerebral blood flow velocity declines before arterial pressure in patients with orthostatic vasovagal presyncope," *J. Am. Coll. Cardiol.* **39**(6), 1039–1045 (2002).
- A. Alshehlee et al., "Incidence and mortality rates of syncope in the United States," *Am. J. Med.* **122**(2), 181–188 (2009).
- D. Sorajja et al., "Syncope while driving clinical characteristics, causes, and prognosis," *Circulation* **120**(11), 928–934 (2009).
- D. Carter et al., "Head-up tilt test for recurrent syncope in pilots," *Aviat., Space Environ. Med.* **76**(12), 1167–1169 (2005).
- S. Matzen et al., "Blood volume distribution during head-up tilt induced central hypovolaemia in man," *Clin. Physiol.* **11**(5), 411–422 (1991).
- K. Sander-Jensen et al., "Hypotension induced by passive head-up tilt—endocrine and circulatory mechanisms," *Am. J. Physiol.* **251**(4), R742–R748 (1986).
- W. Colier et al., "Cerebral and circulatory haemodynamics before vasovagal syncope induced by orthostatic stress," *Clin. Physiol.* **17**(1), 83–94 (1997).
- R. Schondorf, J. Benoit, and T. Wein, "Cerebrovascular and cardiovascular measurements during neurally mediated syncope induced by head-up tilt," *Stroke* **28**(8), 1564–1568 (1997).
- A. F. Folino, "Cerebral autoregulation and syncope," *Prog. Cardiovasc. Dis.* **50**(1), 49–80 (2007).
- J. J. Van Lieshout et al., "Syncope, cerebral perfusion, and oxygenation," *J. Appl. Physiol.* **94**(3), 833–848 (2003).
- R. Cheng et al., "Noninvasive optical evaluation of spontaneous low frequency oscillations in cerebral hemodynamics," *Neuroimage* **62**(3), 1445–1454 (2012).
- M. Marinoni et al., "Technical limits in transcranial Doppler recording: inadequate acoustic windows," *Ultrasound Med. Biol.* **23**(8), 1275–1277 (1997).
- A. Duncan et al., "Optical pathlength measurements on adult head, calf and forearm and the head of the newborn infant using phase resolved optical spectroscopy," *Phys. Med. Biol.* **40**(2), 295–304 (1995).
- P. Madsen et al., "Near-infrared spectrophotometry determined brain oxygenation during fainting," *Acta Physiol. Scand.* **162**(4), 501–507 (1998).
- K. Krakow et al., "Simultaneous assessment of brain tissue oxygenation and cerebral perfusion during orthostatic stress," *Eur. Neurol.* **43**(1), 39–46 (2000).
- E. Y. Joo et al., "Cerebral blood flow abnormalities in patients with neurally mediated syncope," *J. Neurol.* **258**(3), 366–372 (2011).
- E. Szufladowicz et al., "Near-infrared spectroscopy in evaluation of cerebral oxygenation during vasovagal syncope," *Physiol. Meas.* **25**(4), 823–836 (2004).
- Y. Shang et al., "Portable optical tissue flow oximeter based on diffuse correlation spectroscopy," *Opt. Lett.* **34**(22), 3556–3558 (2009).
- Y. Shang et al., "Cerebral monitoring during carotid endarterectomy using near-infrared diffuse optical spectroscopies and electroencephalogram," *Phys. Med. Biol.* **56**(10), 3015–3032 (2011).
- Y. Shang et al., "Diffuse optical monitoring of repeated cerebral ischemia in mice," *Opt. Express* **19**(21), 20301–20315 (2011).
- N. Roche-Labarbe et al., "Noninvasive optical measures of CBV, StO₂ (2), CBF index, and rCMRO₂ in human premature neonates' brains in the first six weeks of life," *Hum. Brain Mapp.* **31**(3), 341–352 (2010).
- G. Yu et al., "Noninvasive monitoring of murine tumor blood flow during and after photodynamic therapy provides early assessment of therapeutic efficacy," *Clin. Cancer Res.* **11**(9), 3543–3552 (2005).
- C. Zhou et al., "Diffuse optical monitoring of hemodynamic changes in piglet brain with closed head injury," *J. Biomed. Opt.* **14**(3), 034015 (2009).

25. G. Yu et al., "Validation of diffuse correlation spectroscopy for muscle blood flow with concurrent arterial spin labeled perfusion MRI," *Opt. Express* **15**(3), 1064–1075 (2007).
26. M. N. Kim et al., "Noninvasive measurement of cerebral blood flow and blood oxygenation using near-infrared and diffuse correlation spectroscopies in critically brain-injured adults," *Neurocrit. Care* **12**(2), 173–180 (2010).
27. F. M. Leonelli et al., "False positive head-up tilt: hemodynamic and neurohumoral profile," *J. Am. Coll. Cardiol.* **35**(1), 188–193 (2000).
28. S. Fantini, M. A. Franceschini, and E. Gratton, "Semi-infinite-geometry boundary-problem for light migration in highly scattering media—a frequency-domain study in the diffusion-approximation," *J. Opt. Soc. Am., B* **11**(10), 2128–2138 (1994).
29. S. O. Rice, "Mathematical analysis of random noise," in *Noise and Stochastic Processes*, N. Wax, Ed., p. 133, Dover, New York (1954).
30. D. A. Boas and A. G. Yodh, "Spatially varying dynamical properties of turbid media probed with diffusing temporal light correlation," *J. Opt. Soc. Am., A* **14**(1), 192–215 (1997).
31. T. Durduran, "Non-invasive measurements of tissue hemodynamics with hybrid diffuse optical methods," PhD Thesis (University of Pennsylvania, 2004).
32. M. Diop et al., "Calibration of diffuse correlation spectroscopy with a time-resolved near-infrared technique to yield absolute cerebral blood flow measurements (vol 2, pg 2068, 2011)," *Biomed. Opt. Express* **3**(6), 1476–1477 (2012).
33. R. Gatto et al., "Frequency domain near-infrared spectroscopy technique in the assessment of brain oxygenation: a validation study in live subjects and cadavers," *J. Neurosci. Methods* **157**(2), 274–277 (2006).
34. Y. Tong and B. D. Frederick, "Time lag dependent multimodal processing of concurrent fMRI and near-infrared spectroscopy (NIRS) data suggests a global circulatory origin for low-frequency oscillation signals in human brain," *Neuroimage* **53**(2), 553–564 (2010).
35. P. C. Njemanze, "Critical limits of pressure-flow relation in the human brain," *Stroke* **23**(12), 1743–1747 (1992).
36. R. Schondorf, J. Benoit, and R. Stein, "Cerebral autoregulation in orthostatic intolerance," *Ann. N. Y. Acad. Sci.* **940**, 514–526 (2001).
37. R. Sheldon et al., "Risk factors for syncope recurrence after a positive tilt-table test in patients with syncope," *Circulation* **93**(5), 973–981 (1996).
38. B. J. Carey et al., "Carbon dioxide, critical closing pressure and cerebral haemodynamics prior to vasovagal syncope in humans," *Clin. Sci.* **101**(4), 351–358 (2001).
39. T. Li, H. Gong, and Q. M. Luo, "Visualization of light propagation in visible Chinese human head for functional near-infrared spectroscopy," *J. Biomed. Opt.* **16**(4), 045001 (2011).
40. T. J. Farrell, M. S. Patterson, and M. Essenpreis, "Influence of layered tissue architecture on estimates of tissue optical properties obtained from spatially resolved diffuse reflectometry," *Appl. Opt.* **37**(10), 1958–1972 (1998).

Biographies of the authors are not available.